Microchimica Acta (2019) 186: 168
https://doi.org/10.1007/s00604-019-3290-3

ORIGINAL PAPER

A copper(II)/cobalt(II) organic gel with enhanced peroxidase-like activity for fluorometric determination of hydrogen peroxide and glucose

Ting Ting Zhao[1] · Zhong Wei Jiang[1] · Shu Jun Zhen[1] · Cheng Zhi Huang[1,2] · Yuan Fang Li[1]

Received: 5 November 2018 / Accepted: 30 January 2019 / Published online: 9 February 2019

Abstract

A bimetallic organic gel was prepared by mixing the bridging ligand 2,4,6-tri(4-carboxyphenyl)-1,3,5-triazine with Cu(II) and Co(II) ions at room temperature. The resulting metal-organic gel (MOG) shows enhanced peroxidase-like activity, most likely due to the synergetic redox cycling between Co(III)/Co(II) and Cu(II)/Cu(I) pairs. These accelerate interfacial electron transfer and generation of hydroxy radicals. The MOG can catalyze the reaction of H_2O_2 with terephthalic acid (TPA), producing a blue fluorescence product with the maximum excitation/emission at 315/446 nm. The enzyme mimic was used to design a fluorometric method for H_2O_2 that has a 81 nM detection limit. H_2O_2 is also formed by glucose oxidase-assisted oxidation of glucose by oxygen, and an assay for glucose was worked out based on the above method. It has a 0.33 μM detection limit. This study may open up a new avenue to design and synthesize nanomaterial-based biomimetic catalysts with multiple metal synergistically enhanced catalytic activity for potential applications in biocatalysis, bioassays and nano-biomedicine.

Keywords Peroxidase mimetic · Redox cycle · Synergistic effect · Metal-organic gel · Enzyme mimic · Terephthalic acid · 2-hydroxyterephthalic acid · Fluorescence · Catalysis · Hydroxy radicals

Introduction

Artificial enzymes imitate the function of natural enzymes by using alternative materials [1, 2]. Nanomaterials, such as gold nanoparticle [3], metal oxide nanoparticle [4–6]and metal organic frameworks [7, 8], as the alternatives of natural enzymes have been found to exhibit unexpected enzyme-like activity with advantage of high stability and low cost. These discovered artificial enzymes have been demonstrated the potential capacity of being applied in bioassay and pharmaceutical processes [9, 10]. To obtain higher enzyme-like activity, the functional assembly strategy of different components will provide new paradigms to enhance properties via the synergic effects. The bimetal nanomaterials, such as Au@Pt [11], Au@Ag [12], Au/CeO_2 [13], Co/2Fe-MOF [14], with improved enzyme-like activity compared to the monometallic analogues have been reported. However, with the mind of further reducing the cost and simplifying the synthesis process, the rational design and synthesis of multicomponent artificial enzymes with enhanced catalytic performance is extremely necessary.

Metal organic gels (MOGs), an analogues of MOFs, formed by self-assembly of metal ions and organic linkers have attracted considerable interest in many fields due to their attracting features, including high surface areas, tunable porosities and inherently present open metal sites [15]. Taking the biggest advantages of easy preparation under mild conditions and good compatibility, so many kinds of MOGs have been prepared and widely used in catalysis [16–18], sensing [19], gas storage [20], drug delivery [21] and environmental

Electronic supplementary material The online version of this article (https://doi.org/10.1007/s00604-019-3290-3) contains supplementary material, which is available to authorized users.

✉ Cheng Zhi Huang
chengzhi@swu.edu.cn

✉ Yuan Fang Li
liyf@swu.edu.cn

[1] Key Laboratory of Luminescent and Real-Time Analytical Chemistry, Ministry of Education, College of Chemistry and Chemical Engineering, Southwest University, Chongqing 400715, People's Republic of China

[2] College of Pharmaceutical Science, Southwest University, Chongqing 400716, People's Republic of China

pollution abatement [22]. In our previous work, Fe-based MOGs with excellent oxidase-like activity was successfully synthesized and applied for the detection of dopamine by catalysis of luminol chemiluminescence [23]. However, as far as we know, the bimetallic organic gel with enzyme-like activity has not been reported up to now. Considering the simplified synthesis steps, low cost and good compatibility, the MOGs are a potential candidate for the preparation of multicomponent nanozymes system.

The Cu/Co bimetallic organic gel (Cu_x/Co_y-MOG) prepared by simple mixing Co^{2+}/Cu^{2+} mixture metal ions and 2,4,6-Tri(4-carboxyphenyl)-1,3,5-triazine (H_3TATAB) in a mild condition was found to show enhanced peroxidase-like activity for the first time (Scheme 1). The synergetic mechanism of redox cycle that between the Co(III)/Co(II) and Cu(II)/Cu(I) pairs was based on the X-ray photoelectron spectroscopy (XPS) and cyclic voltammetry measurements. Additionally, based on this artificial enzymatic reaction system, it was successfully applied to detect H_2O_2 and glucose with satisfactory results. This work may provide a highly promising strategy for reasonable design and synthesis of bimetallic-based nanozymes with high performance via simple process.

Experimental section

Chemicals and apparatus

2,4,6-Tri(4-carboxyphenyl)-1,3,5-triazine (H_3TATAB) was purchased from Na Qian Chemistry Co., Ltd. (Shanghai, China, http://xinxiang62376378.cn.zhsho.com/). Terephthalic acid (TPA) was obtained from Aladdin Chemistry Co., Ltd. (Shanghai, China, http://aladdin.company.lookchem.cn/). Cupric (II) chloride dihydrate ($CuCl_2{\cdot}2H_2O$), cobalt (II) chloride hexahydrate ($CoCl_2{\cdot}6H_2O$) were obtained from Tianjin Hygain Chemical (Group) Co., Ltd. (Tianjin, China, http://tianjinhg2008.51pla.com/). Glucose, L-galactose, pectinose, mannose, fructose, maltose, and sucrose, and 30% (*v*/*v*) H_2O_2 were purchased from Sinopharm Chemical Reagent Co. Ltd. (Shanghai, China, https://www.instrument.com.cn/netshow/SH101458/). All reagents were analytical grade and commercial, and without further purification. The serum samples were kindly provided by Southwest university hospital.

An S-4800 scanning electron microscope (SEM) (Hitachi, Japan) was used to imaging the morphology of Cu_x/Co_y-MOG. Transmission electron microscopic (TEM) characterization was performed on JEOL JEM-1200EX TEM instrument (JEOL, Japan). The xerogels were obtained by a Cool safe 110–4 freeze-drying apparatus (Labogene, Denmark). Powder X-ray diffraction (PXRD) patterns were collected on a D8ADVANCE X-ray diffractometer (Bruker, Germany) with Cu Kα radiation (λ = 1.5406 Å) at a scan rate of 3.00° min^{-1}. Cyclic voltammetric measurement was performed on a CHI 660E electrochemical workstation (CH Instruments, Shanghai, China). A conventional three-electrode cell was constructed with modified glassy carbon electrode (GCE) as working electrode, Pt wire as counter electrode and Ag/AgCl electrode as reference electrode. F-2500 fluorescence spectrophotometer (Hitachi, Tokyo, Japan) was used for fluorescence measurement. The instrument settings as follows: λex = 315 nm (slit 5 nm), λem = 446 nm (slit 5 nm), PMT detector voltage = 400 V. A pH-510 digital pH-meter with a combined glass electrode (California, USA) was performed to test pH. The water used in all the experiments was purified by a Milli-Q system (Millipore, USA).

Preparation of Cu_x/Co_y metal-organic gels (MOG)

Typically, 200 mg (0.46 mmol) of H_3TATAB was dissolved in 10 mL ultrapure water (containing 200 μL triethylamine (TEA)) to prepare stock solution. The stock solution of Co^{2+} and Cu^{2+} were prepared by dissolving $CuCl_2{\cdot}2H_2O$ (0.46 mmol, 79 mg) and $CoCl_2{\cdot}6H_2O$ (0.46 mmol, 109 mg) in 10 mL ultrapure water, respectively. For the synthesis of MOGs, mixture metal ion solution with variable ratio of Cu/Co (from 1:0 to 0:1, while maintaining the total concentration was 0.046 M) was simply mixed with equal volume H_3TATAB (0.046 M). After standing 15 min at room temperature, a series of Cu_x/Co_y-MOG were obtained. To quantify it expediently, the Cu_x/Co_y-MOG were further treated by lyophilization to obtain xerogel.

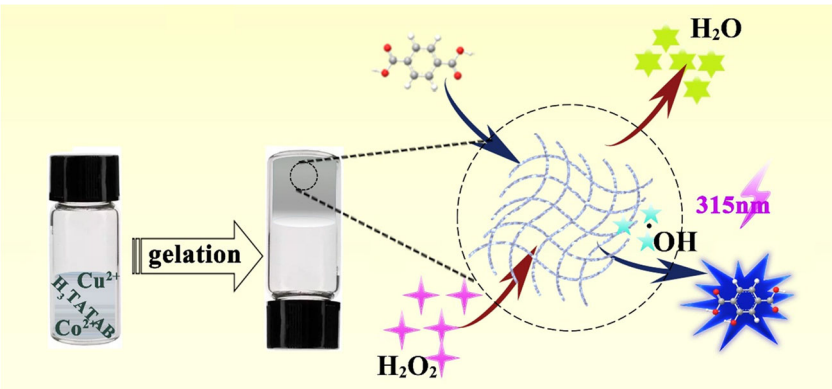

Scheme 1 Schematic illustration of synthesis of Cu_x/Co_y-MOG bimetallic gel and the catalytic activity towards the reaction of H_2O_2 with terephthalic acid

Preparation of serum samples

The samples were first treated by spin dialysis at 10000 rpm for 45 min, and then the eluents were diluted with phosphate buffer (PB, 10 mM, pH 7.0) before measurements.

Determination of hydrogen peroxide and glucose

The $Cu_{0.5}/Co_{0.5}$-MOG (0.2 mg·mL^{-1}, 50 μL), TPA (20 mM, 50 μL) and H_2O_2 with different concentrations were orderly added into 300 μL of phosphate buffer (pH 7.0), and the mixture was diluted with ultrapure water to a volume of 500 μL. After incubating at 45 °C for 20 min, fluorescence spectra were measured under the excitation wavelength of 315 nm.

The detection of glucose was carried out as follows: Typically, GOx (1 mg·mL^{-1}, 50 μL) and 50 μL glucose with different concentrations were added into 300 μL of phosphate buffer (pH 7.0), and incubated at 37 °C for 20 min. TPA (20 mM, 50 μL) and $Cu_{0.5}/Co_{0.5}$-MOG solution (0.2 mg·mL^{-1}, 50 μL) were added to the above glucose reaction solution for another 2 h at 45 °C. The resulting reaction solution was measured by using F-2500 fluorescence spectrometer under the excitation wavelength of 315 nm and detecting the emission intensity at 446 nm. For the detection of glucose in serum, the serum eluents were used instead of glucose solution.

Results and discussion

Choice of materials

As previously reports, the peroxidase-like activities of many nanomaterials, especially noble metal nanoparticles, may be negatively affected by non-specific absorption [2]. Besides, noble metal nanomaterials are prone to aggregate in complex systems, thus reducing their catalytic activity [6, 24]. What's more, the preparation process is usually costly and complicated. Therefore, it is necessary to find a high-efficiency artificial nanoenzyme with low-cost and simple preparation process. MOG is a new kind of metal-organic hybrid materials, which can be prepared by simply mixing the metal ions with the ligand. Furthermore, the catalytic activity can be tuned by changing the metal ions. In our research, the common transition metal ions (such as Cr^{3+}, Mn^{2+}, Fe^{3+}, co^{2+}, Ni^{2+}, cu^{2+}, Zn^{2+}) had been applied for the preparation of MOG. However, only cu^{2+}, co^{2+} and Fe^{3+} can form stable gel with H_3TATAB. The comparation of peroxidase-like activity of the MOGs indicated the Cu(II)/Co(II) bimetallic organic gel shows the best catalytic performance (Fig.S1). Therefore, Cu(II)/Co(II) bimetallic organic gel was selected as a peroxidase-mimetic to further explore their high catalytic activity and application.

Characterization of material

A series of Cu_x/Co_y-MOG can be formed in a wide range molar ratio of Cu^{2+}/Co^{2+}, demonstrating Cu_x/Co_y-MOG displays good compatibility (Fig. S2a-k). Taking $Cu_{0.5}/Co_{0.5}$-MOG as an example, the morphology of the MOGs was firstly examined by SEM and TEM (Fig. 1 a-f). It clearly revealed the MOGs were constructed by nanofibers. The uniform distribution of the elements C, O, N, Co and Cu in the $Cu_{0.5}/Co_{0.5}$-MOG nanofibers were evidenced by the elemental mapping (Fig.1g). There were no obvious diffraction spots except diffraction ring in selected area electron diffraction (SAED) pattern, indicating the amorphous structure of $Cu_{0.5}/Co_{0.5}$-MOG (Fig. 1h). The Brunauer-Emmett-Teller (BET) isotherm disclosed that the as-fabricated MOGs exhibit typical type-III isotherm characteristics of microporous materials (Fig. S3a, b). Furthermore, it also shows that the addition of cobalt ions reduced the BET surface area to a certain extent but with similar aperture distribution. The thermogravimetric analysis (TGA) revealed that the Cu-MOG and $Cu_{0.5}/Co_{0.5}$-MOG show high thermal stability with slow weight losses at a broad range of temperature compared with Co-MOG (Fig. S4) [25]. From the IR spectra, the stretching vibration of C=O in H_3TATAB was shift from 1697 cm^{-1} to 1604 cm^{-1}, indicating that the metal ions and carboxyl groups were ligated via coordinate bond (Fig. S5) [25]. The powder XRD patterns of $Cu_{0.5}/Co_{0.5}$-MOG are like those of the monometallic Cu-MOG and Co-MOG, revealing that these materials possess similar structure(Fig. S6). Furthermore, two diffraction peaks at 22.01° and 23.84° can be observed, which are matched well with the previous reported MOGs, assigning to the π-π stacking [26, 27].

Peroxidase-like activity of the Cu_x/Co_y-MOG

A typical TPA-H_2O_2 reaction was employed as a model reaction to explore the peroxidase-like activity of the Cu_x/Co_y-MOG. As shown in Fig. 2, almost no fluorescence signal can be measured from the H_2O_2 + TPA system (curve a), suggesting that the reaction of H_2O_2 and TPA can hardly happen in the absence of enzyme. The weak fluorescent was observed in the presence of Co-MOG (curve b), showing that Co-MOG had a weak mimic enzyme activity. The high catalytic activity can be observed in Cu-MOG and $Cu_{0.5}/Co_{0.5}$-MOG enzymatic reaction system, demonstrating the Cu(II) is the major catalytic activity center. Moreover, the peroxidase like activity of the Cu/Co-MOGs with various molar ratios of Cu/Co was also evaluated (Fig. S7a, b). It clearly shows that the catalytic activity highly depended upon the Cu/Co ratio. Particularly, the $Cu_{0.5}/Co_{0.5}$ is the optimum molar ratio to achieve the best peroxidase-like activity.

As we know, non-fluorescent TPA can be oxidized by •OH into the 2-hydroxyterephthalic acid (TAOH) which shows a

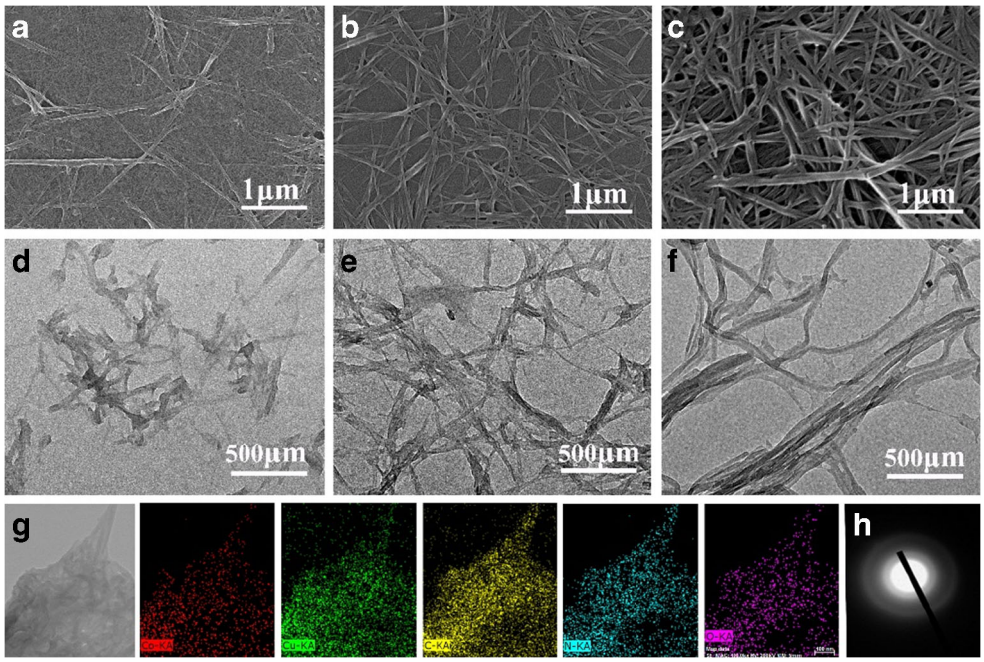

Fig. 1 SEM images of Cu-MOG, $Cu_{0.5}/Co_{0.5}$-MOG and Co-MOG (**a-c**), and the corresponding TEM images (**d-f**); (**g**) the TEM and elemental mapping images of $Cu_{0.5}/Co_{0.5}$-MOG for Co, Cu, C, N and O with color superposition; (**h**) the SAED pattern of $Cu_{0.5}/Co_{0.5}$-MOG

strong fluorescence with the maximum excitation/emission at 315/446 nm. Therefore, the thiourea as •OH scavenger and electron spin resonance (ESR) study were applied as a direct method to verify the production of •OH (Fig. S8a, b). The results showed that the the fluorescence signal of TAOH can be decreased more than 95% by the presence of 2mM of thiourea, and the the typical quartet characteristic peak in ESR spectrum with relative intensities 1:2:2:1 was observed, indicating that $Cu_{0.5}/Co_{0.5}$-MOG can induce •OH production by catalysing H_2O_2.

Mechanism exploration

Based on the above experimental results, the bimetallic $Cu_{0.5}/Co_{0.5}$-MOG shows higher peroxidase-like activity than Cu-MOG and Co-MOG. To explore the mechanism that able to justify the superior performance of $Cu_{0.5}/Co_{0.5}$-MOG, the X-ray photoelectron spectroscopy (XPS) was performed to characterize the change of valence state of metal component before and after reacting with H_2O_2 (Fig. 3a). The high-resolution Cu2p XPS spectrums of $Cu_{0.5}/Co_{0.5}$-MOG before and after treating with H_2O_2 (Fig. 3b, c) both show main peaks at roughly 934.5 eV and 954.3 eV, which originated from the Cu(II) in Cu2p-O bonds. [24] Besides, the Cu LMM Auger spectra were performed to distinguish the valence states of the Cu species (Fig. 3d). It shows an obvious shift of Auger peak from 570.6 eV to 571.8 eV after H_2O_2 treatment, confirming that the formation of Cu(I) in the $Cu_{0.5}/Co_{0.5}$-MOG after reacting with H_2O_2. [28, 29] The XPS patterns and data analysis of Co species were displayed in Fig. 3e, f and Table S1, respectively. The spin-orbit splitting $\Delta E(2p_{1/2}\text{-}2p_{3/2})$ was changed from 15.9 eV to 15.4 eV, and the significantly reduced Σsat/ICo2p$_{3/2}$ value were observed after treating with H_2O_2, demonstrating the presence of Co(III) component [30, 31].

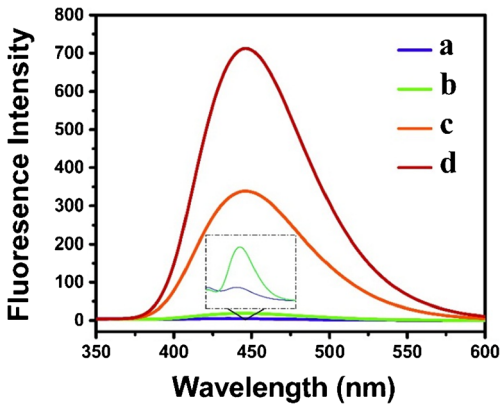

Fig. 2 Fluorescence spectra of (**a**) H_2O_2 + TPA, (**b**) H_2O_2 + TPA + Co-MOG, (**c**) H_2O_2 + TPA + Cu-MOG and (**d**) H_2O_2 + TPA+ $Cu_{0.5}/Co_{0.5}$-MOG. The concentrations of H_2O_2, TPA and the MOGs were 8μM, 2mM, 20 mg·L^{-1}, respectively; insert showed the amplified of (**a**) and (**b**). λ_{ex}: 315 nm; λ_{ex}:446 nm; slits:5nm; voltage:400V

According to previous reports, the catalytic mechanism of Cu(II) and Co(II) can be described in the following reactions: [32–34]:

$$Co(II) + H_2O_2 \rightarrow Co(III) + \bullet OH + OH^- \quad (1)$$

$$Cu(II) + H_2O_2 \rightarrow Cu(I) + \bullet O_2H + H^+ \quad (2)$$

$$Cu(I) + H_2O_2 \rightarrow Cu(II) + \bullet OH + OH^- \quad (3)$$

As described above, a synergetic catalytic mechanism of $Cu_{0.5}/Co_{0.5}$-MOG was proposed as follows: 1) once H_2O_2 was added, •OH radicals were generated by active sites including Cu(II) and Co(II) on the catalyst surface, resulting the

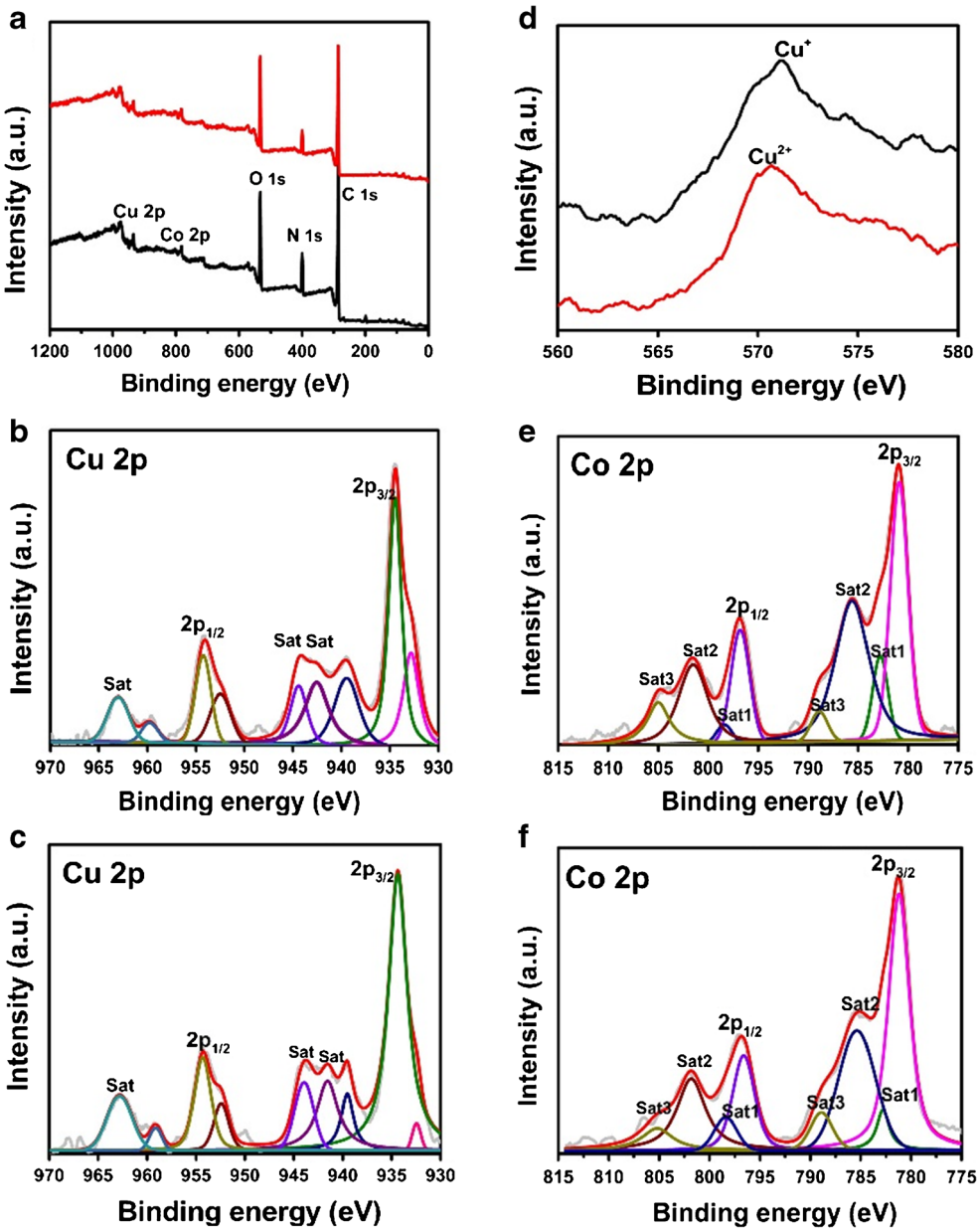

Fig. 3 **a** High resolution XPS spectra of $Cu_{0.5}/Co_{0.5}$-MOG before (black line) and after (red line) treat with H_2O_2. Wide spectra and high-resolution spectra of (**b**) Cu2p of $Cu_{0.5}/Co_{0.5}$-MOG without H_2O_2 treatment, (**c**) Cu2p of $Cu_{0.5}/Co_{0.5}$-MOG after H_2O_2 treatment, (**d**) Cu LMM Auger spectra of $Cu_{0.5}/Co_{0.5}$-MOG before (red line) and after (black line) treat with H_2O_2, (**e**) Co2p of $Cu_{0.5}/Co_{0.5}$-MOG without H_2O_2 treatment, (**e**) Co2p of $Cu_{0.5}/Co_{0.5}$-MOG after treat with H_2O_2

generation of Cu(I) and Co(III); 2) according to cyclic voltammogram and eq. (6) (Fig. S9 and Table 1), the Cu(I) oxidation by Co(III) is thermodynamically feasible, which is conducive to the redox cycles of Cu(II)/Cu(I) and Co(III)/Co(II) via single electron transfer. This process can accelerate the interfacial electron transfer within $Cu_{0.5}/Co_{0.5}$-MOG. Therefore, the synergetic effect caused by the endogenous redox cycle of Cu(II)/Cu(I) and Co(III)/Co(II) pairs is benefit for the more •OH generation (Fig. 4).

Hydrogen peroxide and glucose detection

As we all know, the enzymatic activity greatly depends on the reaction condition, such as concentration of catalyst and substrate, pH and temperature. The optimization of experimental conditions is displayed in Fig. S10. Under the optimal reaction conditions, the typical fluorescence response was observed in the presence of different concentrations H_2O_2, and the fluorescence intensity versus hydrogen peroxide

Table 1 The reaction potentials from cyclic voltammogram curve of $Cu_{0.5}$/ $Co_{0.5}$-MOG

Electrode Reaction	E (V vs NHE)	
Co(III) + e → Co(II)	0.076	(4)
Cu(I) – e → Cu(II)	0.624	(5)
Co(III) + Cu(I) → Cu(II) + Co(II)	0.700	(6)

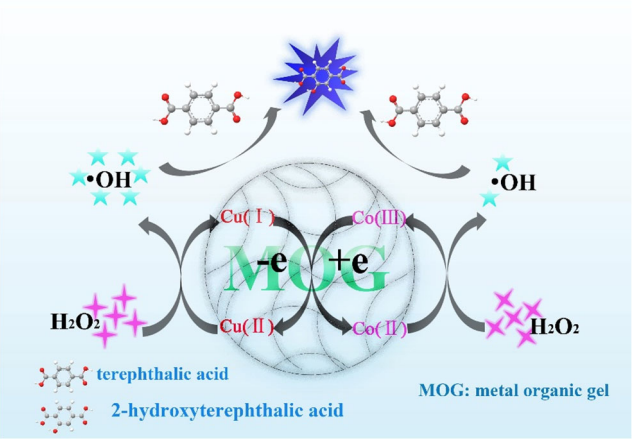

Fig. 4 Possible mechanism for $Cu_{0.5}/Co_{0.5}$-MOG as artificial enzyme

concentration was linear over the range from 1.0 μM to 10 μM. The linear regression equation was $F = 100.54\ c\text{-}81.72$ ($R^2 = 0.997$) (where F is the fluorescence intensity and c is the concentration of H_2O_2, respectively.) The limit of detection was approximately 81 nM ($S/N = 3$) (Fig. 5a, b). As shown in Fig. S11, it clearly demonstrated that the common ions did not affect the detection of H_2O_2. Moreover, the $Cu_{0.5}/Co_{0.5}$-MOG was used for determination of glucose combining with glucose oxidase. As Fig. 5c shown, the fluorescence intensity increased markedly along with the increase of glucose concentration. Good linear relationship was obtained in the range of 0.5 μM to 120 μM. The linear regression equation was $F = 5.453\ c\text{-}0.2424$ ($R^2 = 0.994$) and the limit of detection was calculated to be 0.33 μM ($S/N = 3$) (Fig. 5d). The selectivity experiment was also carried out with a satisfactory result (Fig. S12). The analytical performance of the method was also compared with other methods based on peroxidase-mimics reported in the literature (Table S2). The present method showed a good linear range and high sensitivity, and it realized the detection of H_2O_2 and glucose at the sub-μM levels.

To confirm the precision and reliability of this method, the standard addition method was performed. The spiked samples were obtained by adding a certain amount of glucose to the dilute serum. Table S3 shows the acceptable recovery rates (98%–108%). This demonstrates that the method can be used for the detection of glucose in serum samples. Besides, the reproducibility of Cu(II)/Co(II) bimetallic organic gel in the glucose oxidase/glucose system was investigated (Fig. S13). The results clearly indicated that no significant loss of activity in the seven successive using, suggesting that the Cu(II)/Co(II) bimetallic organic gel possesses long-term stability and reproducibility. On the other hand, the morphology of Cu(II)/Co(II) bimetallic organic gel in different systems has been studied by SEM (Fig. S14). The results show the morphology of Cu(II)/Co(II) bimetallic organic gel has no serious changes in different systems.

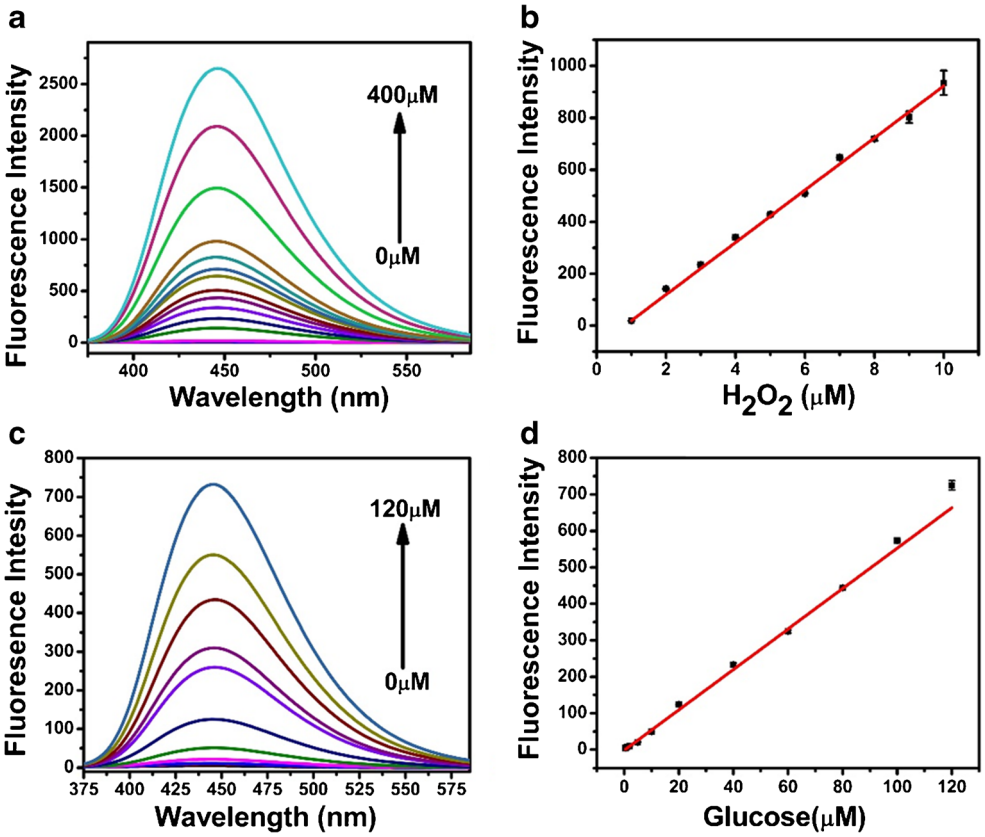

Fig. 5 **a** Fluorescence spectra of $Cu_{0.5}/Co_{0.5}$-MOG + TPA with various concentrations of H_2O_2 from 0 to 400 μM in phosphate buffer (pH 7.0); (**b**) Plot of the fluorescence intensity of $Cu_{0.5}/Co_{0.5}$-MOG + TPA against the concentrations of H_2O_2, insert: the linear calibration plot for H_2O_2; (**c**) Fluorescence spectra of $Cu_{0.5}/Co_{0.5}$-MOG + TPA + GOx with various concentrations of glucose from 0 to 120 μM; (**d**) Linear calibration plot for glucose. λ_{ex}: 315 nm; λ_{ex}:446 nm; slits:5nm; voltage:400V

Conclusions

In summary, the $Cu_{0.5}/Co_{0.5}$-MOG with enhanced peroxidase-like activity has been designed and synthesized successfully. The excellent performance was attributed to the synergistic effect of endogenous redox cycle that between Cu(II)/Cu(I) and Co(III)/Co(II) pairs, leading more generation of •OH. Subsequently, the $Cu_{0.5}/Co_{0.5}$-MOG was successfully applied to fluorescent detection of glucose in serum. We believe that this study would light a new beacon for the design and synthesis of peroxidase-like enzyme, and may stimulate new development in this field. The potential applications of Cu_x/Co_y-MOG in bioassay, environmental remediation, and catalysis are also expected to be broadened.

Acknowledgements The authors are grateful to the National Natural Science Foundation of China (NSFC, No. 21575117).

Compliance with ethical standards The author(s) declare that they have no competing interests.

References

1. Wei H, Wang E (2013) Nanomaterials with enzyme-like characteristics (nanozymes): next-generation artificial enzymes. Chem Soc Rev 42(14):6060–6093
2. Chen J, Chen Q, Chen J, Qiu H (2016) Magnetic carbon nitride nanocomposites as enhanced peroxidase mimetics for use in colorimetric bioassays, and their application to the determination of H_2O_2 and glucose. Microchim Acta 183(12):3191–3199
3. Zhan L, Li CM, Wu WB, Huang CZ (2014) A colorimetric immunoassay for respiratory syncytial virus detection based on gold nanoparticles-graphene oxide hybrids with mercury-enhanced peroxidase-like activity. Chem Commun 50(78):11526–11528
4. Hu AL, Deng HH, Zheng XQ, Wu YY, Lin XL, Liu AL, Xia XH, Peng HP, Chen W, Hong GL (2017) Self-cascade reaction catalyzed by CuO nanoparticle-based dual-functional enzyme mimics. Biosens Bioelectron 97:21–25
5. Chang Q, Deng K, Zhu L, Jiang G, Yu C, Tang H (2009) Determination of hydrogen peroxide with the aid of peroxidase-like Fe_3O_4 magnetic nanoparticles as the catalyst. Microchim Acta 165(3–4):299–305
6. Choleva TG, Gatselou VA, Tsogas GZ, Giokas DL (2017) Intrinsic peroxidase-like activity of rhodium nanoparticles, and their application to the colorimetric determination of hydrogen peroxide and glucose. Microchim Acta 185(1):22
7. Wang S, Deng W, Yang L, Tan Y, Xie Q, Yao S (2017) Copper-based metal-organic framework nanoparticles with peroxidase-like activity for sensitive colorimetric detection of Staphylococcus aureus. ACS Appl Mater Interfaces 9(29):24440–24445
8. Chen WH, Vazquez-Gonzalez M, Kozell A, Cecconello A, Willner I (2018) Cu^{2+}-modified metal-organic framework nanoparticles: a peroxidase-mimicking Nanoenzyme. Small 14(5):1–8
9. Zhang Z, Zhang X, Liu B, Liu J (2017) Molecular imprinting on inorganic Nanozymes for hundred-fold enzyme specificity. J Am Chem Soc 139(15):5412–5419
10. Huang H, Liu L, Zhang L, Zhao Q, Zhou Y, Yuan S, Tang Z, Liu X (2017) Peroxidase-like activity of ethylene diamine Tetraacetic acid and its application for ultrasensitive detection of tumor biomarkers and circular tumor cells. Anal Chem 89(1):666–672
11. He W, Liu Y, Yuan J, Yin JJ, Wu X, Hu X, Zhang K, Liu J, Chen C, Ji Y, Guo Y (2011) Au@Pt nanostructures as oxidase and peroxidase mimetics for use in immunoassays. Biomaterials 32(4):1139–1147
12. He W, Wu X, Liu J, Hu X, Zhang K, Hou S, Zhou W, Xie S (2010) Design of AgM bimetallic alloy nanostructures (M = au, Pd, Pt) with tunable morphology and peroxidase-like activity. Chem Mater 22(9):2988–2994
13. Bhagat S, Srikanth Vallabani NV, Shutthanandan V, Bowden M, Karakoti AS, Singh S (2018) Gold core/ceria shell-based redox active nanozyme mimicking the biological multienzyme complex phenomenon. J Colloid Interface Sci 513:831–842
14. Yang H, Yang R, Zhang P, Qin Y, Chen T, Ye F (2017) A bimetallic (co/2Fe) metal-organic framework with oxidase and peroxidase mimicking activity for colorimetric detection of hydrogen peroxide. Microchim Acta 184(12):4629–4635
15. Sutar P, Maji TK (2016) Coordination polymer gels: soft metal-organic supramolecular materials and versatile applications. Chem Commun 52(52):8055–8074
16. Lee JH, Kang S, Lee JY, Jung JH (2012) A tetrazole-based metallogel induced with ag+ in catalysis. Soft Matter 8:6557–6563
17. Hassan HM, Näther C, Winkler HC, Janiak C (2012) Highly selective and "green" alcohol oxidations in water using aqueous 10% H_2O_2 and iron-benzenetricarboxylate metal-organic gel. Inorg Chim Acta 391:75–82
18. Ke F, Li Y, Zhang C, Zhu J, Chen P, Ju H, Xu Q, Zhu J (2018) MOG-derived porous FeCo/C nanocomposites as a potential platform for enhanced catalytic activity and lithium-ion batteries performance. J Colloid Interface Sci 522:283–290
19. Lin Q, Sun B, Yang Q-P, Fu Y-P, Zhu X, Wei T-B, Zhang Y-M (2014) Double metal ions competitively control the guest-sensing process: a facile approach to stimuli-responsive supramolecular gels. Chem Eur J 20(36):11457–11462
20. Zhu X, Zheng H, Wei X, Lin Z, Guo L, Qiu B, Chen G (2013) Metal-organic framework (MOF): a novel sensing platform for biomolecules. Chem Commun 49(13):1276–1278
21. TZ G, C O, Osuji JD, Forster ER, Dufresne LR (2010) Stimuli-responsive smart gels realized via modular protein design. J Am Chem Soc 132:14024–14026
22. Okesola BO, Smith DK (2016) Applying low-molecular weight supramolecular gelators in an environmental setting-self-assembled gels as smart materials for pollutant removal. ChemSocRev 45(15):4226–4251
23. He L, Peng ZW, Jiang ZW, Tang XQ, Huang CZ, Li YF (2017) Novel iron(III)-based metal-organic gels with superior catalytic performance toward Luminol Chemiluminescence. ACS Appl Mater Interfaces 9(37):31834–31840
24. Xiong Y, Qin Y, Su L, Ye F (2017) Bioinspired synthesis of Cu^{2+}-modified covalent Triazine framework: a new highly efficient and promising peroxidase mimic. Chem EurJ 23:11037–11045
25. Aiyappa HB, Saha S, Garai B, Thote J, Kurungot S, Banerjee R (2014) A distinctive PdCl2-mediated transformation of Fe-based Metallogels into metal-organic frameworks. Cryst Growth Des 14(7):3434–3437
26. Roy S, Katiyar AK, Mondal SP, Ray SK, Biradha K (2014) Multifunctional white-light-emitting metal-organic gels with a sensing ability of nitrobenzene. ACS Appl Mater Interfaces 6(14):11493–11501
27. Peng ZW, Yuan D, Jiang ZW, Li YF (2017) Novel metal-organic gels of bis(benzimidazole)-based ligands with copper(II) for electrochemical selectively sensing of nitrite. Electrochim Acta 238:1–8

28. Kirsch PD, Ekerdt JG (2001) Chemical and thermal reduction of thin films of copper (II) oxide and copper (I) oxide. J Appl Phys 90(8):4256–4264
29. Poulston S, Parlett PM, Stone P, Bowker M (1996) Surface oxidation and reduction of CuO and Cu_2O studied using XPS and XAES. Surf Interface Anal 24:811–820
30. Ribeiro RS, Silva AMT, Figueiredo JL, Faria JL, Gomes HT (2017) The role of cobalt in bimetallic iron-cobalt magnetic carbon xerogels developed for catalytic wet peroxide oxidation. Catal Today 296:66–75
31. Ivanova T, Naumkin A, Sidorov A, Eremenko I, Kiskin M (2007) X-ray photoelectron spectra and electron structure of polynuclear cobalt complexes. J Electron Spectrosc Relat Phenom 156:200–203
32. Lin JM, Shan XQ, Hanaoka SC, Yamada M (2001) Luminol Chemiluminescence in unbuffered solutions with a cobalt(II)-ethanolamine complex immobilized on resin as catalyst and its application to analysis. Analchem 73:5043–5051
33. Wang Y, Zhao H, Li M, Fan J, Zhao G (2014) Magnetic ordered mesoporous copper ferrite as a heterogeneous Fenton catalyst for the degradation of imidacloprid. Appl Catal B Environ 147:534–545
34. Zhang L, Nie Y, Hu C, Qu J (2012) Enhanced Fenton degradation of rhodamine B over nanoscaled cu-doped $LaTiO_3$ perovskite. Appl Catal B Environ 125:418–424